Bulg. J. Phys. **31** (2004) 135–147

Application of Real-Time SAXS, WAXS, DSC, and PLM Methods for Investigation of Structure and Phase Transitions of Poly(heptane-1,7-dyil-4,4'-biphenyldicarboxylate)*

G. K. Todorova[1], **M. N. Kresteva**[1], **M. Iliev**[1], **E. Pérez**[2], **J. M. Pereña**[2], **A. Bello**[2], **M. Shlouf**[3]

[1]University of Sofia, Faculty of Physics, Department of General Physics; 5, James Bourchier Blvd., 1164 Sofia, Bulgaria

[2]Instituto de Ciencia y Technologia de Polimeros (CSIC) Juan de la Cierva, 3 28006 Madrid, Spain

[3]Institute of Macromolecular Chemistry (CAS), 2 Heyrovskeho nam., 16206 Prague 6, Czech Republic

Received *23 April 2003*

Abstract. A number of methods were applied to investigate the structure and phase transitions of poly(heptane-1,7-dyil-4,4'-biphenyldicaroboxilate). Monotropic smectic phase transition was observed. Complete transformation from an isotropic melt to smectic phase was suggested whereas the transition from smectic to crystalline phase is only partial. Conclusions about the nature and kinetics of the observed phase transitions were made. Structural model was proposed based on the comprehensive analysis of all applied methods.

PACS number: 61.30Eb, 61.30.Vx, 64.70Mv, 83.80Xz

1 Introduction

Liquid crystalline materials attract great attention in the last decades because of their broad spectrum of applications as well as the challenge of deeper understanding of such systems. Liquid crystalline polymers, instead of using low-molar-mass compounds, will provide materials with good electrical and optical properties but possessing better mechanical stability.

Main-chain liquid crystalline polymers have a monomer consisting of rigid mesogen (able to form a mesophase) and flexible spacer, both as parts of the

*This work is dedicated to Professor, DSci, Alexander Derzhanski, Corresponding Member of Bulgarian Academy of Sciences, on the occasion of his 70th Anniversary.

backbone. The final formed structure is in consequence of the competition between the self-organization of mesogens and the polymer conformation.

Series of studies, devoted to investigations on poly(bibenzoate) (*PBB*) series with all-methylene spacer, where the number of carbons in the spacer (n) varies from 3 to 22, are available in the literature [1-22]:

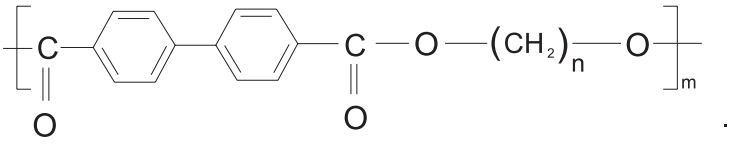

Homologues with n=3–9 on cooling from an isotropic state form smectic (S) mesophase followed by a transformation into crystalline (C) structure [2-4,7,8,15,16-18,21]. On heating, only members with $n < 7$ exhibit a transition back from C to S phase and then S phase melts [2,3,21]. When n is between 7 and 9 the crystalline structure melts directly [15,16,21]. Members with n=10–12 do not form a mesophase and they crystallize directly from the melt [8,13]. Members with higher number of methylene groups in the spacer show complex behavior *i.e.* they are able to form more ordered mesophases as well as various crystalline structures [9,12].

General tendency of PBB series is that transition temperatures tend to decrease when the number of methylene units increases [2-4,7,21 and papers therein]. Well-expressed "even–odd" effect has been observed [2-4,7,21]. The even homologues have higher transition temperatures, glass transition temperatures, enthropies and smectic layer spacings, than their odd neighbors. More extended conformations were established for even- while for odd-members the valence angles force the macromolecules to adopt a less extended conformations [3,4,7,16,21].

Very important difference between even- and odd- members of the PBB series exists [2-21]. The type of smectic structure is quite different. Even-members form smectic A (S_A) with both axes of the polymer chain and rigid units lying perpendicular to the layers. In contrast, when n is odd smectic CA (S_{CA}) is formed. The molecular axes are perpendicular to the mesogenic layers but the rigid units are tilted towards the layers normal, at the same absolute angular value but in opposite directions into the adjacent layers [4,7,21].

Poly(heptane-1,7-dyil-4,4'-biphenyldicarboxylate) (*P7MB*) is a PBB series member with seven methylene units in the spacer. On cooling from a isotropic melt, it forms a S_{CA} mesophase, followed by partial transformation into a crystalline phase. On subsequent heating, the mesophase is not observed and the partially crystalline material melts directly [15,16,21], *i.e.* it shows a monotropic behavior.

2 Material

P7MB was synthesized by melt transesterification, as reported previously [15]. Its inherent viscosity, measured in chloroform at 25°C, was 1.03 dL/g. The molecular weight, determined by gel permeation chromatography (GPC) is: $M_w = 78000$ and $M_w/M_n = 2.86$. Glass transition temperature (T_g) is 41°C [23].

3 Experimental

Time resolved X-ray experiments were carried out at the Synchrotron in Daresbury, UK, and at Synchrotron "DESY", Hamburg, Germany. Non-isothermal processes were followed during cooling (2°C/min, 10°C/min) and heating (10°C/min, 12°C/min). The intervals of the scattering vector, $s = \dfrac{2\sin\vartheta}{\lambda}$, where:

- $0.02 < s < 0.5$ nm^{-1} — Small Angle X-ray Scattering (*SAXS*), where one peak is observed on cooling after S–C transition and during heating. It originates from the quasi-periodic arrangement of the crystalline lamellar stacks (Figures 1a, b)
- $0.5 < s < 1$ nm^{-1} — Middle Angle X-ray Scattering (*MAXS*), One scattering peak is observed, which is attributed to the first order of diffraction in direction perpendicular to the mesogenic layers (Figures 1c, d)
- $1.2 < s < 3.4$ nm^{-1} — Wide Angle X-ray Scattering (*WAXS*); Scattering from the amorphous phase, as well as from the smectic and crystalline domains is observed (Figures 1e, f).

Phase transitions of P7MB were detected by Differential Scanning Calorimetry (*DSC*). DSC measurements were carried out on Perkin-Elmer DSC-7 calorimeter at cooling rates (v_c) from 2°C/min to 20°C/min and heating rate (v_h) 10°C/min.

Polarized light microscopy (*PLM*) microphotographs were taken using optical microscope (Zetopan Pol, Reichert) equipped with heating stage (Mettler FP52/FP5, allowing heating/cooling rates 0.2, 1, 2, 3 and 10 °C/min), objective with extra-large working distance (40/0.55 160/0-2.5 ELWD, Nikon) and a digital camera (DXM1200, Nikon, maximum resolution 3840×2998 pixels). Samples were sliced with a razor blade, set between two supporting glasses, placed into heating stage and melted so that a thin transparent layer of the sample was obtained; this layer was observed with optical microscope. All microphotographs were taken with crossed polarizers. Brightness and contrast were adjusted at the beginning of the observation and were not varied during heating/cooling runs.

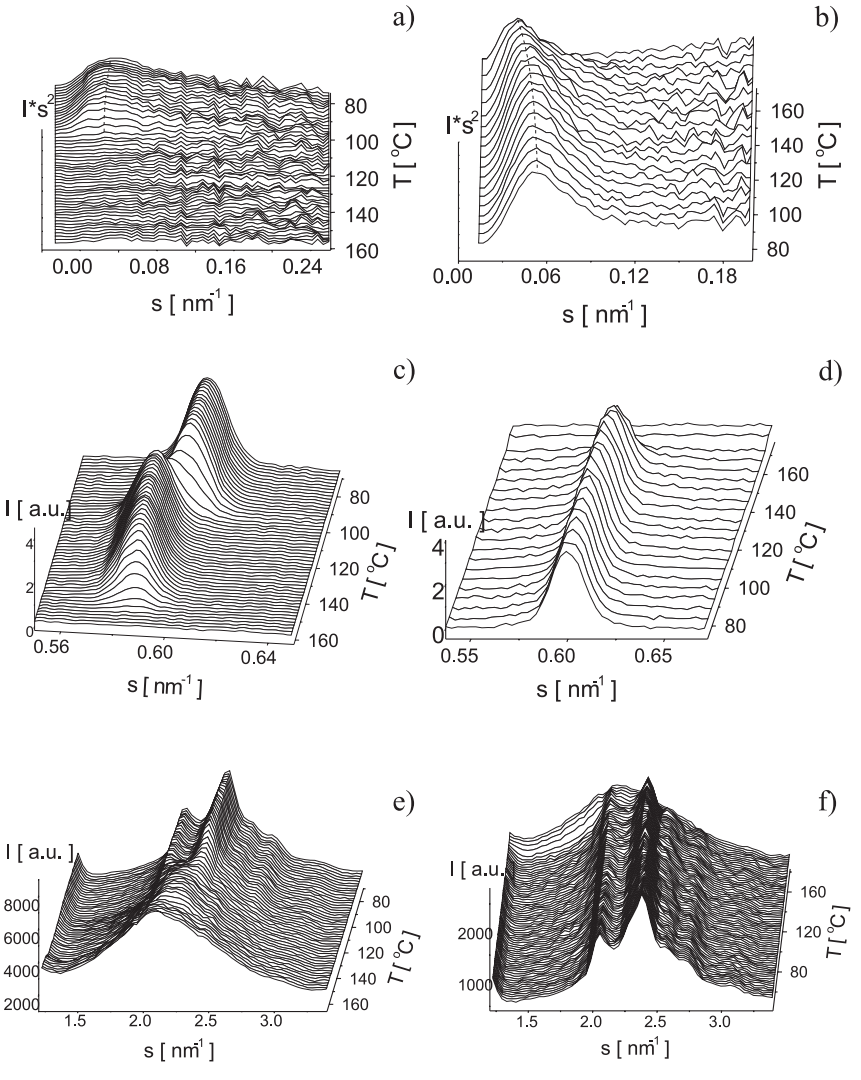

Figure 1. Lorentz corrected SAXS profiles: a) cooling with 10°C/min from an isotropic melt and b) subsequent heating with 10°C/min; MAXS peak profiles: c) cooling with rate 10°C/min and d) subsequent heating with 10°C/min; WAXS patterns: e) cooling with 2°C/min and f) subsequent heating with 12°C/min.

4 Results and Discussion

DSC thermograms were recorded at different cooling rates in an interval from 2°C/min to 20°C/min and subsequent heating with 10°C/min. In Figure 2, DSC

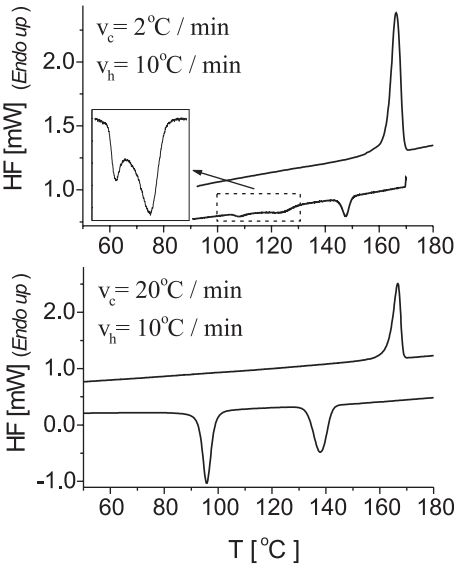

Figure 2. DSC curves of P7MB, starting with cooling from an isotropic melt and subsequent heating: cooling rate 2°C/min (upper plot) and 20°C/min (bottom plot), for both the heating rate is $v_h = 10°$C/min. HF is the heat flow.

traces for lowest and highest cooling rates are shown. Two phase transitions are clearly seen on cooling whereas on heating only one transition is presented. The transitions were recognized as isotropic melt (I)–S_{CA} and S_{CA}–C on cooling and only one transition on heating as C–I.

4.1 Isotropic Melt – Smectic Transition

The high temperature exotherm in DSC thermograms is attributed to an $I - S_{CA}$ phase transition [2,3,15,21]. Its enthalpy is $\Delta H_1 \approx 15.8$ J/g independent of the cooling rate [24].

Transition is ruled by the molecular asymmetry [25], leading to a separation of heterogeneous units on nanoscale. Driving forces of the formation of S phase are cohesive forces between equal and repulsive between unlike species. The existence of critical temperature for nanophase separation, T_{ns}, has been suggested [26].

Upon cooling from an isotropic state, the transition into a smectic phase is manifested by the growth of a diffraction peak at $s \approx 0.587$ nm^{-1} (1.705 nm), originating from the smectic layer periodicity, d_s (Figure 1c) and a shift to the larger s values in a liquid-like diffuse scattering in WAXS pattern, d_{AM}. The maximum of the peak of the amorphous halo is centered at $s \approx 2.164$ nm^{-1}

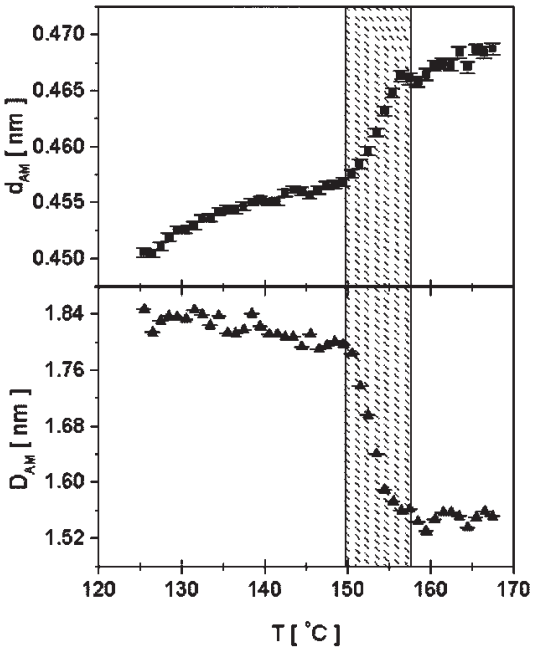

Figure 3. d-spacing of amorphous halo in WAXS patterns during cooling from an isotropic melt with a rate 2°C/min. Transition interval is marked with the rectangle.

(0.462 nm), which is characteristic of interchain packing correlation (Figure 1e and Figure 3a). During transition, the average interchain distance, calculated from the position of the amorphous peak decreases stepwise (Figure 3a) and the correlation length derived from the half width of the halo, D_{AM}, increases (Figure 3b).

PLM microphotographs of the polymer textures at different temperatures during cooling are shown in Figure 4. The I–S_{CA} transition starts at about 148°C (Figure 4a) in a good agreement with the DSC and X-ray results. At lowering the temperature after S phase formation, the microtexture remains the same. Only phase boundaries become sharper and the brightness of the domains increases (Figures 4b and c).

SAXS peak is not observed. One has to suppose a complete transformation from isotropic melt to smectic phase as it has been done for the PBB series member with $n = 5$ [13].

Based on PLM results, despite of the SAXS-peak lack, we assume that the domains with folded chains are formed during I–S transition. Folding is considered to arise from the counterbalance between the energy lost and entropy gain [5,7-9,11,13,27]. The size of the domains, D_s, has been roughly estimated of

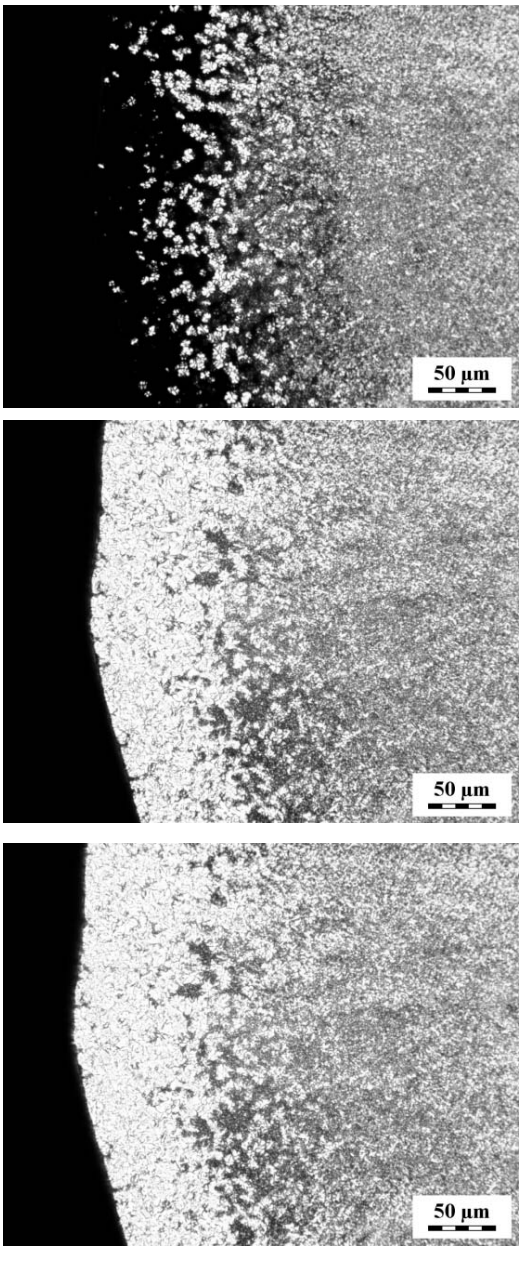

Figure 4. Polarized light micrographs taken during cooling with a rate $v_c = 3^\circ$C/min: a) $T = 148^\circ$C (onset of I–S transition); b) $T = 135^\circ$C (smectic phase); c) $T = 70^\circ$C.

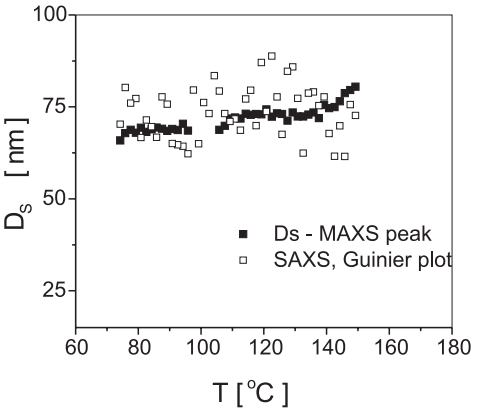

Figure 5. Temperature dependence of Domain dimensions, D_s, derived from MAXS peak (filled squires) and SAXS patterns (open squires) during cooling with a rate $v_c = 10^{\circ}$C/min.

about 50–70 nm depending on the exact experimental conditions [28,29] and applied experimental method. In Figure 5, the derived D_s values by means of two different techniques are shown. First one is using a half width of the MAXS peak, ϖ, ($D_s = 1/\varpi$) and the second one applying the Guinier's law in the SAXS region at $s \to 0$ ($I(s) = I_0 \exp(-(R_g s)^2/3)$ where R_g is the radius of gyration of crystallites and I is the observed SAXS intensity. We consider that $R_g \approx D_s$).

4.2 Smectic- Crystalline Phase Transition

The second DSC exotherm, corresponding to S_{CA}–C transition, since six crystalline peaks over the halo appear and grow on WAXS patterns (Figure 1e lowest temperature interval). Their temperature dependencies are discussed elsewhere [28]. This exotherm consists of two overlapping components (Figure 2). Noteworthy, the sum of both enthalpies ($\Delta H_2 \approx 19.4$ J/g) [24] is independent of applied cooling rate.

In the mean time, MAXS peak changes its position to the value of about 1.67 nm [28]. There are many possibilities about the way of phase transformation. We have been discussed them in another our work [28]. The most reasonable one is that during crystallization S and C phases exist simultaneously and the process itself modifies the S_{CA} phase [17,28]. Phase transformation occurs within the already existed smectic domains (D_s is constant before and after transition, see Figure 5).

Degree of crystallinity increases step-wise during the phase transformation up to about $X_{cr}^{WAXS} = 0.22$ [28], derived from WAXS patterns. The crystallization

in this sense is not complete even if it takes place from the already ordered S phase. The same result has been obtained by Tokita *et al.* in the case of PBB with $n = 5$ [13].

During the transition, the phase contrast between present phases increases, giving rise to a SAXS peak growth. It has an average value of about 15 nm (Figure 1a).

4.3 Crystalline – Isotropic melt phase transition

On heating, DSC thermogram displays only one transition. It has enthalpy $\Delta H_1 \approx 32$ J/g.

During heating from the semi-crystalline state no peculiarities are observed in MAXS and WAXS regions. MAXS as well as all WAXS peaks are preserved up to the melting interval (See Figures 1d, f). Their d-spacings slightly increase due to the temperature expansion [28].

One SAXS peak is seen during the heating as a result of scattering from quasi-periodic packing of crystalline lamellae separated by the disordered phase layers. The electron density distribution is a Fourier transformation of SAXS scattering intensity [30-32]. One-dimensional correlation function analysis was used to determine the structural parameters [30-32]. In the case of two phases with sharp interface, the one-dimensional correlation function is: $\gamma_1(x) = \frac{\int_0^\infty I(s)s^2\cos(2\pi xs)ds}{\int_0^\infty I(s)s^2 ds}$ [32] and Long period, L, thickness of the crystalline lamellae, l_{cr}, thickness of the disordered layers, l_{am}, and linear degree of crystallinity, X_{cr}^{SAXS} could be derived. Based on scanning electron microscopy (*SEM*) results [33], the lamellar stacking has been proved and one could use the afore-mentioned model.

Figure 6 presents the temperature dependences of L, l_c and l_a. The exponential increase in all parameters is observed. The long period increases manly due to changes within the disordered phase. X_{cr}^{SAXS} is of about 0.27 in a good agreement with the WAXS results [28].

An important feature of the structure is the significant deviations from Porod's law $\left(\lim_{s\to\infty} I(s) = I_b(s) + \frac{K}{s^m}\right)$ [30-32]. For both cooling and heating the Porod's slope, m (Figure 7), is less than this one predicted for the ideal two-phase system ($m = 4$). Ruland has considered possible deviations from the Porod's law [34] as a result of either diffuse interface between the phases or anisotropic fluctuations within them. In our opinion and according to the analysis proposed by Ruland, the two-dimensional fluctuations within the phases have to be supposed [29].

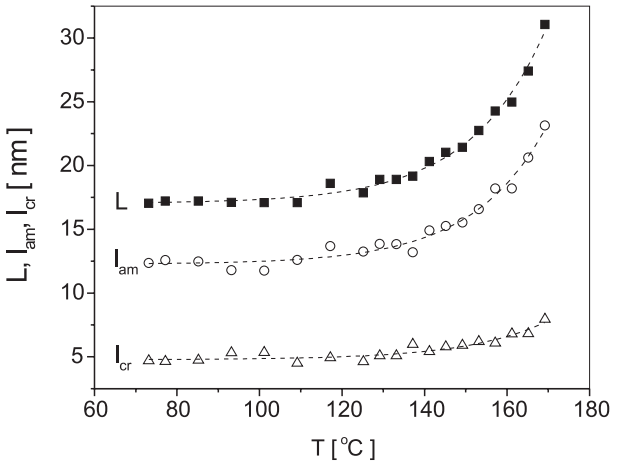

Figure 6. Temperature dependencies of structural parameters, derived from one-dimensional correlation function analysis: Long period, L (solid squires), crystalline lamellar thickness, l_{cr} (open triangles), and thickness of disordered layers, l_{am} (open circles). Heating with a rate $v_h = 10^{\circ}$C/min [29].

Polymer crystals could melt in two different ways:

1) Surface melting, during which transition layer increases, crystal core becomes smaller and smaller, until the full isotropization. The surface melting is in contradiction of our experimental results, as the average crystal sizes in both directions, perpendicular and parallel to the molecular axes, increases with the temperature.

2) The density fluctuations appear within the crystal phase until the free energy of the crystal phase equals to those of the disordered phase. This assumption is in agreement with our results. Hence, the melting process has more probably a fluctuation nature rather than to be caused by surface melting.

Let us compare the domain dimensions (D_s, see Figure 5) and long period (L, see Figure 6). D_s is in order of about 50–70 nm whereas the L is in order of 15–32 nm. Even more, l_{cr} is very low – only several nm (4–6 nm). This observation allows us to suggest the electron density distribution in direction perpendicular to the macromolecular axes. Hence the final model of P7MB could be assumed as shown in Figure 8. The domains consist of chain folded lamellae with thickness D_s and the electron density distribution periodicity is in direction perpendicular to the chain axes.

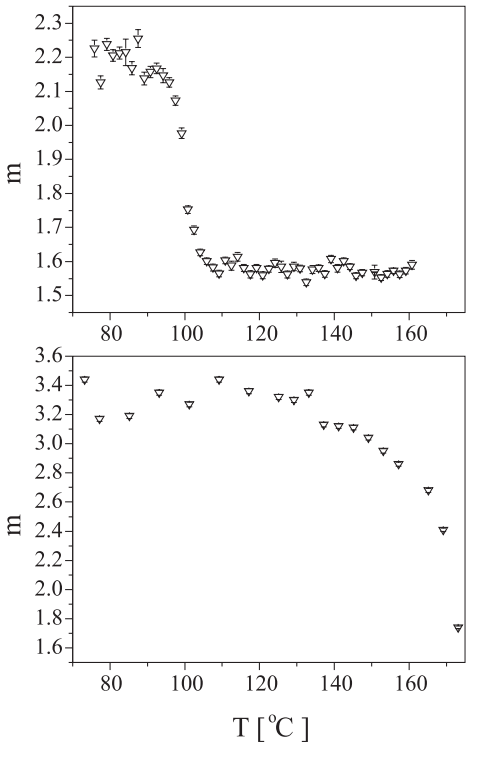

Figure 7. Temperature dependence of Porod's slope, m, a) during cooling with a rate $v_c = 10^{\circ}$C/min and b) heating with $v_h = 10^{\circ}$C/min [29].

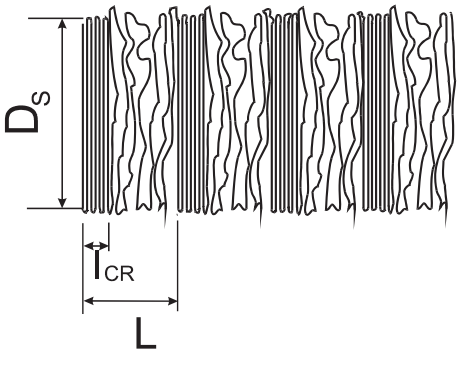

Figure 8. Structural Model of P7MB.

5 Conclusion

All applied methods confirm the appearance of a monotropic smectic phase on cooling of P7MB.

The I–S transition on cooling from melt is ruled by nanophase separation and the critical temperature T_{ns} exists. The well-defined domains with folded chains are formed. The overall transformation is observed.

Further cooling causes S–C transition. In the transition range, the S and C phases coexist. Crystallization takes place within the already formed S domains and the process modifies the S phase. At low temperatures modified S and C phases are present and the crystallinity is relatively low.

On subsequent heating, the final semi-crystalline structure is preserved up to the melting interval. The significant deviations from Porod's law are evidence for two-dimensional fluctuations within the phases, which amount increase exponentially in the melting interval.

Model with periodic electron density distribution in the perpendicular to the macromolecular axes direction is proposed, based on the comprehensive analysis of all obtained results.

References

[1] J. Watanabe, W.R. Krigbaum (1984) *Macromolecules* **12** 2288.

[2] J. Watanabe, M. Hayashi (1988) *Macromolecules* **21** 278.

[3] J. Watanabe, M. Hayashi (1989) *Macromolecules* **22** 4083.

[4] J. Watanabe, M. Hayashi, A. Morita, T. Niori (1994) *Mol. Cryst. Liq. Cryst.* **254** 221.

[5] M. Tokita, T. Takahashi, M. Hayashi, K. Inomata, J. Watanabe (1996) *Macromolecules* **29** 1345.

[6] J. Watanabe, M. Hayashi, M. Tokita (1996) *Reactive & Functional Polymers* **30** 191.

[7] J. Watanabe, M. Hayashi, Y. Nakata, T. Niori, M. Tokita (1997) *Prog. Polym. Sci.* **22** 1053.

[8] M. Tokita, K. Osada, J. Watanabe (1997) *Liq. Cryst.* **23** 453.

[9] M. Tokita, K. Osada, M. Yamada, J. Watanabe (1998) *Macromolecules* **31** 8590.

[10] M. Tokita, K. Osada, J. Watanabe (1998) *Liq. Cryst.* **24** 477.

[11] M. Tokita, K. Osada, S. Kawauchi, J. Watanabe (1998) *Polym. Journal* **8** 687.

[12] M. Tokita, M. Sone, H. Kurosu, I. Ando, J. Watanabe (1998) *Journal of Mol. Structure* **446** 215.

[13] M. Tokita, K. Osada, J. Watanabe (1998) *Polym. Journal* **30** 589.

[14] K. Osada, H. Niwano, M. Tokita, S. Kawauchi, J. Watanabe (2000) *Macromolecules* **33** 7420.

[15] E. Pérez, A. Bello, M.M. Marugán, J.M. Pereña (1991) *Polym. Communications* **31** 386.

[16] A. Bello, E. Riande, E. Pérez, M.M. Marugán, J.M. Pereña (1993) *Macromolecules* **26** 1072.

[17] E. Pérez, M.M. Marugán, D.L. VanderHart (1993), *Macromolecules* **26** 5852.

[18] A. Bello, J.M. Pereña, E. Pérez, R. Benavente (1994) *Macrom. Symp.* **84** 297.

[19] R. Benavente, Zhen Zhu, J.M. Pereña, A. Bello, E. Pérez (1996) *Polymer* **37** 2379.

[20] N.J. Heaton, R. Benavente, E. Pérez, A. Bello, J.M. Pereña (1996) *Polymer* **37** 3791.

[21] E. Pérez, J.M. Pereña, R. Benavente, A. Bello (1997) *Handbook of Engineering Polymeric Materials*, Ed. by N.P. Cheremisinoff, Marsel Dekker, Inc.

[22] J.M. Pereña, R. Benavente, M.M. Marugán, E. Pérez, A. Bello (1998) *Polymer* **39** 5671.

[23] J. M. Pereña, M. M. Marugán, A. Bello, E. Pérez (1991) *J. Noncryst. Solids* **891** 131.

[24] G. Todorova, M. Kresteva, E. Pérez, J. M. Pereña, A. Bello, "*Phase transitions of liquid crystalline polyesters. Popy(heptamethylene p,p'-bibenzoate)*, in press.

[25] A. Petrov (1999) *The Lyotropic State of Matter: Molecular Physics and Living Matter Physics*, Gordon & Breach Publishers, Inc., L.-N.Y. -Ph., Ch. 3, pp 87-130; R.P. Rang, W.A. Pasegian (1973) *Biochim Biophys. Acta* **318** 299.

[26] M. Kresteva, G. Todorova, E. Pérez, M.M. Marugán, J.M. Pereña, *Phase transitions of liquid crystalline polyesters. Popy(heptane-1,7-dyil-4,4'-biphenyldicarboxylate)*, in press.

[27] P.G. de Gennes (1982) *Pol. Liq. Cryst.*, Ed. A. Chifferi, W.R. Krigbaum, and R.B. Mayer, New York Academic Press, 124.

[28] G. Todorova, M. Kresteva, E. Pérez, J.M. Pereña, A. Bello, *Structure and phase transitions of poly(hepamethylene p,p'-bibenzoate). II. WAXS and DSC studies*, in press.

[29] G. Todorova, M. Kresteva, E. Perez, J.M. Pereña, A. Bello, *Structure and phase transitions of poly(hepamethylene p,p'-bibenzoate). II. SAXS, DSC and SEM studies*, in press.

[30] G. Strobl (1996) *The Physics of Polymers, Concept of understanding their structure and behavior*, Springler.

[31] O. Glatter and O. Kratki (1982) *Small Angle X-ray scattering*, Alder Press.

[32] B. Goderis, H. Reynaers, M.H.J. Koch, V.B.F. Mathot (1999) *J. Polym. Sci.: Part B: Polym. Phys* **37** 1715.

[33] To be published.

[34] W. Ruland (1970) *J. Appl. Cryst.* **4** 70.